Are Grignard Reactions in Deep Eutectic Solvents Interface-Driven?

Iva Manasi,[†[a,b]] Marco Bortoli, [† [c]] Daniel T. Bowron,[[d]] Mario Campana,[[d]] Oliver S. Hammond,[[e]] Thomas F. Headen,[[d]] Jake Hooton,[[b]] Eva Hevia[[f]], Michele Cascella,*[[c]] Odile Eisenstein[[c,g]] and Karen J. Edler*[[b,h]]

[a] Department of Physics, University of Bristol, Tyndall Avenue, Bristol, BS8 1TL, UK.

[b] Department of Chemistry, University of Bath, Claverton Down, Bath, BA2 7AX, UK.

[c] Department of Chemistry and Hylleraas Centre for Quantum Molecular Sciences, University of Oslo, PO Box 1033 Blindern, 0315 Oslo, Norway.

[d] ISIS Neutron and Muon Source, Rutherford Appleton Laboratory, Oxford, OX11 0QX, UK.

[e] European Spallation Source ERIC, Kongens Lyngby 2800, Denmark.

[f] Department für Chemie und Biochemie, Universität Bern, Freiestrasse 3, 3012 Bern, Switzerland.

[g] ICGM, Université de Montpellier, CNRS, ENSCM, 1919 Route de Mende, 34293 Montpellier, France.

[h] Department of Chemistry Centre for Analysis and Synthesis (CAS) Lund University, Lund, 221 00 Sweden.

Corresponding author e-mails: karen.edler@chem.lu.se, michele.cascella@kjemi.uio.no

† joint first authors

* corresponding authors

Abstract

Organolithium and organomagnesium addition reactions to ketones are important and versatile processes used in synthetic organic chemistry. However, due to the high reactivity of these species, the reactions are usually done under an inert atmosphere at low temperature. Recent work has demonstrated the possibility to carry out these procedures safely on the benchtop, in air at room temperature using deep eutectic solvents (DES) to dissolve the organic substrate. Surprisingly the organometallic reagent, added in an organic solution, is compatible with these unconventional conditions, and instead of undergoing fast decomposition by the DES, better yields and selectivities are observed than when working under standard conditions. Earlier it was posited that the choline chloride component of the DES might chemically activate the ketone substrate making it more amenable to reaction. Here we probe this hypothesis with experiments; liquid diffraction, neutron reflectometry, NMR and interfacial tension measurements for acetophenone in DES and with all-atom molecular dynamics simulations. We show instead that the role of the choline chloride is to reduce the solubility of the ketone, forcing it to accumulate at the air-solvent (or organic solvent/DES) interface. Molecular dynamics simulations for

isopropyl magnesium chloride in the same DES/tetrahydrofuran bi-phase system also indicate a preference to localize at the interface. These results suggest that surface accumulation promotes the addition reaction and account for these remarkable experimental conditions. Accumulation of the organic non-protic substrate at the interface could also protect the organometallic species from rapid decomposition by the protons of the DES.

Introduction

Deep eutectic solvents (DES) are room-temperature liquids formed by molecular mixtures with a lower melting point at the eutectic composition relative to that predicted by ideal mixing.[1, 2] They have a 'liquid window' of compositions around the eutectic composition, which makes them attractive and applicable as general-purpose solvents.[1, 3] DES can show high thermal stability, non-flammability and low vapour pressure, therefore low volatility.[2] Typical DES components (e.g. choline chloride, urea, natural carboxylic acids, amino acids and carbohydrates, polyalcohols, etc.) can be obtained from renewable sources and are gaining interest as solvents to replace volatile organic solvents in electrochemistry, and organic synthesis as well as preparation of nanoparticles[4] and dissolution of biomolecules.[5]

DES have recently been shown to contribute uniquely to reaction chemistry and syntheses for a range of components.[6] Organolithium and organomagnesium (Grignard) addition reactions to ketones are one of the most versatile and fundamental methods to generate new C-C bonds, allowing formation of tertiary alcohols.[7-9] Traditionally these reagents need to be used under inert atmosphere conditions, using dry and degassed organic solvents, with strict control of the temperature. Breaking new ground in this area, in 2014 Garcia-Alvarez and Hevia *et al*[9] reported the chemoselective alkylation of ketones by RMgX and RLi reagents in water-containing DES exposed to air, at room temperature - conditions normally incompatible with polar organometallics. Yet, in some DES, these reactions resulted in improved yields and better selectivities than when using conventional inert atmosphere protocols. Moreover, they were less energy intensive, markedly more environmentally friendly, and safer. In particular, choline chloride:glycerol (ChCl:Gly) and choline chloride:water (ChCl:W) solvents had a stabilizing effect, allowing high yields for alkylation reactions even in the presence of air. The reaction between RMgX, added in an ether solution, and the substrate in DES occurs within seconds. The organomagnesium or organolithium react preferentially with the substrates rather than the DES components, despite these containing OH groups that are known to react rapidly with such reagents. On the contrary, attempts to carry out the same reactions on glycerol or water alone were not successful, demonstrating the importance

of the DES to facilitate these C-C bond forming processes.[10] Similar effects occurred in chemoselective nucleophilic arylation/alkylations of non-activated imines.[10] Interestingly, despite these synthetic advances, the exact role of the DES still remains unclear, although previous experimental studies have hinted at some type of substrate activation involving the ketone and the ammonium salt choline chloride, a component of the DES employed.

Our aim in this work is to provide experimental structural characterization of a choline chloride:glycerol (1:2) DES solution containing acetophenone (AcPh) as model ketone substrate. In addition, we have integrated the data with a computational model of this solution, also in phase co-existence with isopropyl magnesium chloride (iPrMgCl) in tetrahydrofuran (THF). In this way, we provide for the first time a detailed molecular picture of this reaction mixture, to investigate the interactions that underpin the beneficial effects.

When RMgX or RLi are added to the DES mixture, they are normally added as a solution in an organic solvent with rapid mixing.[11] Further experiments by the Hevia group have identified the importance of efficient mixing in obtaining the high selectivity and yields observed in these reactions.[11, 12] This, together with our initial experiments using wide-angle scattering to probe the solvation of substrates and reaction products in the DES, suggest a direct role of the liquid/liquid interface in promoting the reactive processes. We report here both wide-angle neutron scattering experiments and further combination of NMR and interfacial techniques, tensiometry and neutron reflectivity, that demonstrate the role played by ChCl:Gly DES in mediating the chemoselective alkylation of ketones. We have compared the dissolution behaviour of acetophenone in ChCl:Gly with that in pure glycerol to understand the role of the choline salt in the observed synthetic outcomes. Measurements of the interface highlight the adsorption of the substrate to the air-DES and organic-DES interface, reaffirming the hypothesis that this is an interfacial reaction. Classical molecular dynamics simulations of solution of AcPh in pure glycerol and in DES further mark the importance of the ionic component of the DES, also pin-pointing the role of the hydrogen bond network in determining AcPh solubility in DES. Furthermore, measurements on biphasic DES/supported organic layers showed the preference of AcPh for the lower polarity organic phase. This is again confirmed by simulations of a complete DES/THF system containing both AcPh and ^{i}PrMgCl (Figure 1), which predicted the migration of all relevant chemical species from their initial bulk phases toward the interface area.

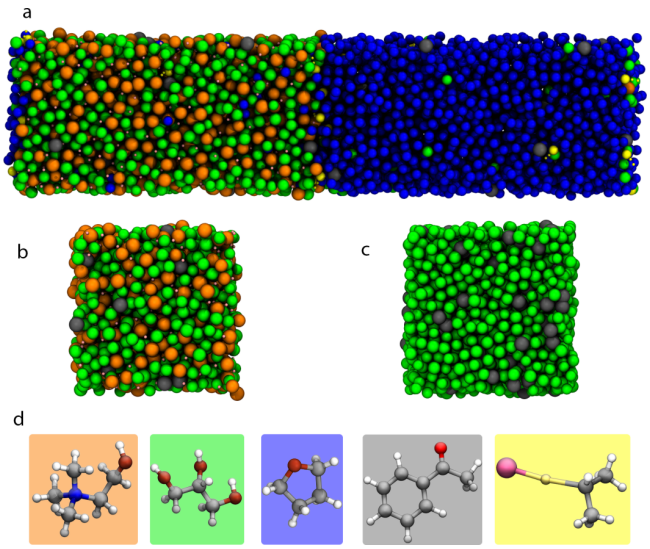

Figure 1: Model depiction of the investigated systems: (a) ChCl:Gly mixed system with THF containing AcPh and iPrMgCl, (b) ChCl:Gly with AcPh, (c) pure Gly with AcPh and (d) atomistic structure of the systems' components. Molecules are represented as beads located at their centre of mass. Colour code: Ch+: orange; Gly: green; THF: blue; AcPh: grey; iPrMgCl: yellow.

Results

Liquid neutron diffraction data was collected from ChCl:Gly DES at a molar ratio of 1 ChCl to 2 glycerol, at 25 °C without and with addition of acetophenone. Isotopic substitution of deuterium for hydrogen in choline chloride, glycerol and acetophenone allowed 6 different solutions to be measured for the ChCl:Gly DES, and 8 different solutions were measured with added acetophenone (see details in Supplementary information section S2). There is good agreement between the experimental data, EPSR models (Figures S4-S6), and the MD simulation results, with the latter giving calculated coordination numbers slightly higher than those obtained from experiment.

Choline chloride: Glycerol (1:2) alone

For the pure DES, without acetophenone, molecular radial distribution functions (RDFs, Figure 2) were calculated between the central atoms of the components, choline, Cl^-, glycerol and acetophenone, using the EPSR model and from MD simulations. The position of the first peak (r_{max}) in the RDFs and the coordination numbers calculated are shown in Table 1. These RDFs (at 25 °C) are comparable to those previously reported for the ChCl:Gly DES measured at 60 °C by Turner and Holbrey (Table S2).[13]

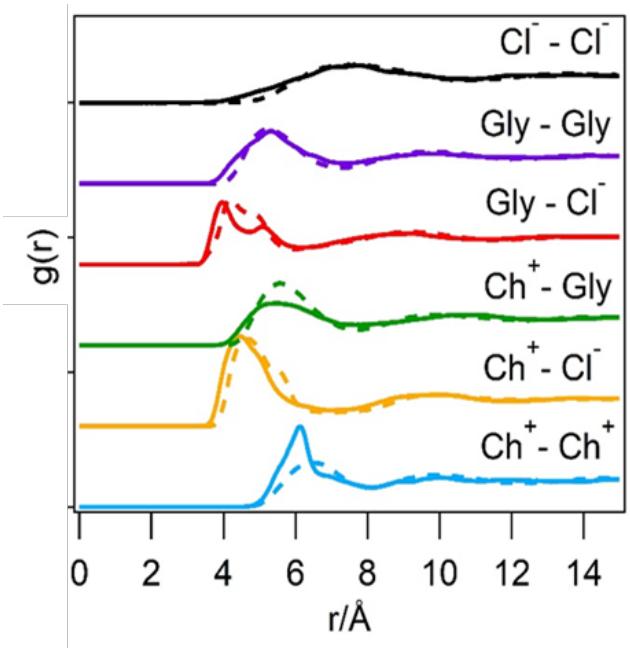

Figure 2: Molecular RDFs for ChCl:Gly DES components from EPSR (solid lines) and MD simulations (dashed lines). The computed RDFs are calculated between representative molecular centroids. The plots are stacked along the y-axis for clarity.

The RDFs for the DES samples show the Ch^+–Cl^- association with a peak at 4.5 Å and the Ch^+–Gly with a peak at 5.6 Å. The Gly–Cl^- peak is at 4.0 Å with a secondary peak at 5.1 Å, showing two distinct Cl^- population centres relative to glycerol, one that is centred at the central carbon (4.0 Å) and another that is centred at the peripheral carbons (5.1 Å). The Gly–Gly RDF has a peak at 5.3 Å falling between the Gly–Cl^- and Gly–Ch^+ peaks. The first Ch^+–Ch^+ peak in the RDF is found at 6.2 Å indicating that this is a second shell association. The RDFs were used to calculate the average coordination number for the specified molecular pairs, from the origin to the nearest neighbour distance (i.e. until the first minima in the RDF). The strongest associations are observed for Gly-Gly with a coordination number of 7.7 ± 2.3 and Ch^+–Gly with a coordination number of 7.7 ± 2.2, which is consistent with the fact that glycerol is more abundant as well as has more H-bonding sites. This is followed by the choline and chloride interactions, where we have charged interactions between the N^+ in choline and Cl^- as well as H-bonding with the OH in choline. The structure of the ChCl:Gly DES is dominated by glycerol-glycerol H-bonding, similar to that present in glycerol. This is concordant with the structure reported by Turner and Holbrey at 60 °C who suggested an extensive, persistent, homo-molecular glycerol hydrogen bonding network for ChCl:Gly DES that is key to formation of the ChCl:Gly DES.[13] A similar structure has also been reported by Faraone et al[14] who suggested that the DES comprises a glycerol H-bonding network with interstitial choline ions. However, the Ch^+–Ch^+ and Gly–Ch^+ peak positions are at lower values in our

studies (room temperature), compared to those observed by Turner and Holbrey at 60°C suggesting that there is more thermal expansion in the choline part of the DES.

Table 1: The position of the first peak (r_{max}) in the radial distribution functions (RDFs) and the coordination numbers (CN) for the various molecules calculated using the COORD routine in EPSR and from MD simulations for the ChCl:Gly DES. The data from Turner and Holbrey[13] is also given for comparison.

RDF	Experimental 25 °C EPSR (this work)		MD (this work)		Experimental 65 °C (Turner & Holbrey[13])	
	Peak (Å)	CN	Peak (Å)	CN	Peak (Å)	CN
Gly-Gly	5.3	7.7 ± 2.3	5.3	6.9 ± 1.8	5.3	7.5 ± 1.7
Gly-Cl^-	4.0	1.9 ± 0.9	4.3	2.2 ± 0.9	4.1	2.0 ± 1.0
Gly-Ch^+	5.6	7.6 ± 2.3	5.6	9.1 ± 1.2	5.9	8.4 ± 1.6
Ch^+-Cl^-	4.5	3.7 ± 1.2	4.7	4.0 ± 1.0	4.1	3.1 ± 1.1
Ch^+-Ch^+	6.2	3.5 ± 1.5	6.4	4.2 ± 1.5	6.5	2.5 ± 0.9
Cl^--Cl^-	7.2	9.7 ± 2.3	7.7	11.3 ± 1.3	7.1	10.1 ± 2.5

Choline chloride: Glycerol (1:2) with AcPh

After measuring the solvent alone, the samples were recovered and acetophenone was added to the mixtures. AcPh had an unexpectedly low solubility in ChCl:gly, compared to that in pure glycerol. Saturated solutions of AcPh in ChCl:gly were prepared and the data were modelled using the actual solution concentration of 0.2 mmol g^{-1} (i.e. 6.7 mol%, ca.2 wt.%), as measured on the recovered solutions by NMR (Figure S1). Empirical Potential Structure Refinement (EPSR) was used, continuously refining the molecular positions against the experimental scattering data obtained at each different composition (results shown in Figures S5). The measured RDFs for the ChCl:Gly DES with acetophenone show no change in peak position or shape for the Ch^+–Ch^+, Ch^+–Cl^-, Ch^+–Gly, Gly–Cl^- or Gly–Gly associations compared to that of the DES (**Error! Reference source not found.**). This indicates that the acetophenone does not alter the associations of different molecules in the DES. The AcPh RDFs show high noise as there are very few AcPh molecules in the simulation, and this uncertainty also causes the larger discrepancy between the MD and EPSR models for this species. The AcPh–Gly peak is at 5.5 Å with a secondary peak at 6.7 Å (Figure 3a) showing AcPh associations with glycerol centred around the central and the peripheral carbons or alternatively interaction of the glycerol with the phenyl ring (π electrons) and with the carbonyl group. The Ch^+–AcPh interactions are at a similar distance with a peak at 5.5 Å and a broad distribution around 6.3 Å again indicating two interactions either with the two H-bonding sites in the choline (ammonium and OH group) or with the π-electrons and the carbonyl group in the

acetophenone. The Cl^-–AcPh associations are at a closer distance of 5.1 Å and the AcPh–AcPh associations are at a similar distance to the Cl^-–AcPh interactions of 5.0 Å with a secondary feature at 7 Å. The strongest associations are observed for AcPh-Gly with a coordination number of 7.6 ± 2.1 followed by choline (coordination number 3.7 ± 1.4) and then chloride (coordination number 2.4 ± 1.2). There are virtually no associations between AcPh–AcPh, as would be expected for such a dilute system. These interactions indicate interstitial accommodation of AcPh in the glycerol H-bonding network of the DES, with the acetophenone strongly interacting with the glycerol and having less preferred interactions with the choline and chloride.

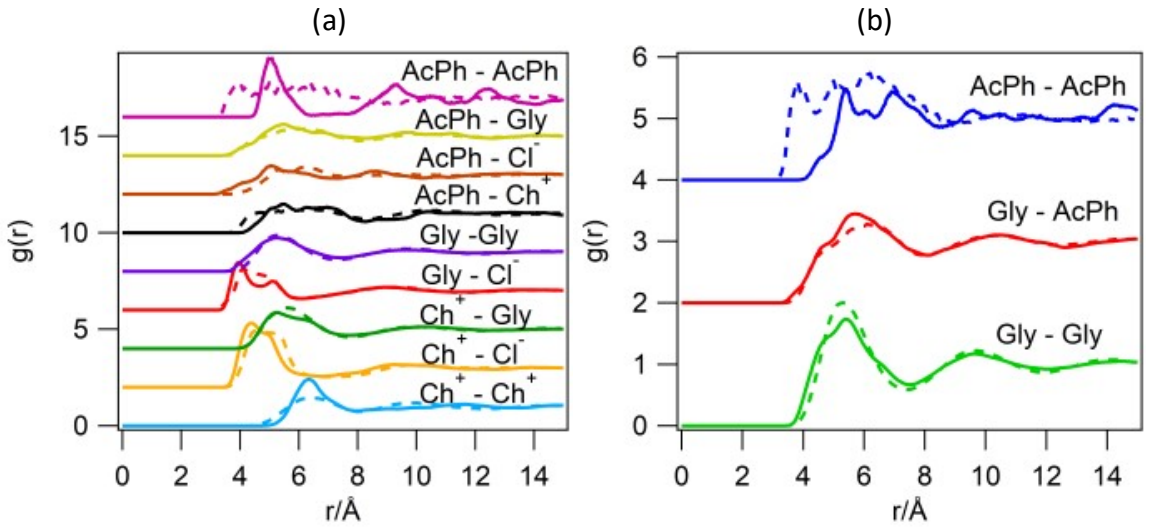

Figure 3: Molecular RDFs for a solution of DES with acetophenone (a), and for a solution of glycerol and acetophenone (b). Molecular RDFs from EPSR are shown by the solid lines, results from MD simulations are shown by the dashed lines. The computed RDFs are calculated between representative molecular centroids. The plots are stacked along the y-axis for clarity.

Glycerol alone with AcPh.

Wide-angle scattering data was also collected for solutions of acetophenone in pure glycerol, shown in Supplementary Information Figure S6. In this case, NMR measurements showed that acetophenone is more soluble in pure glycerol than in ChCl:Gly DES (Supplementary Information Figure S2). Therefore, the scattering data was modelled in EPSR using the measured AcPh concentration of 0.75 mmol g^{-1}. The RDFs for glycerol with acetophenone show the Gly-Gly peak at 5.4 Å, similar to the distance for Gly-Gly associations observed for the ChCl:Gly DES and for glycerol alone by Towey et al.[15] The AcPh-Gly association peak is also at 5.4 Å with a shoulder at 6.3 Å (Figure b). This is similar to the observation for

AcPh-Gly associations in ChCl:Gly DES. These could be due to associations around the central and the peripheral carbons in glycerol or with the phenyl ring and carbonyl group in acetophenone. The AcPh-AcPh interactions have high noise due to the small number of acetophenone molecules in the simulation, and have a broad peak at ~6 Å. The AcPh-AcPh associations here are stronger compared to those in ChCl:Gly DES, having a coordination number of 1.2 ± 0.9, and as expected there are more associations of Gly to AcPh, (coordination number of 14.0 ± 2.0), similar to the total coordination number of glycerol, choline and chloride in the DES, suggesting that the choline chloride interactions with AcPh are replaced by glycerol-AcPh interactions in pure glycerol solutions. The larger coordination number of AcPh-AcPh could potentially be due to the higher concentration of acetophenone dissolved in glycerol (0.75 mmol g^{-1}) compared to the ChCl:Gly DES (0.2 mmol g^{-1}), a factor of 3.75. The interactions are however at similar length scales and of similar strength.

Table 2: The position of the first peak (r_{max}) in the radial distribution functions (RDFs) and the coordination numbers (CN) for the various molecules calculated using the COORD routine in EPSR and from MD simulations for a 0.2 mmol g^{-1} (6.7 mol%) solution of AcPh in ChCl:Gly DES and for a 0.75 mmol g^{-1} solution of AcPh in pure Gly.

RDF	DES				Gly			
	EPSR		MD		EPSR		MD	
	Peak (Å)	CN	Peak (Å)	CN	Peak (Å)	CN	Peak (Å)	CN
Gly-Gly	5.3	7.2 ± 2.1	5.3	6.7 ± 1.9	5.4	8.3 ± 2.3	5.3	12.5 ± 1.7
Gly-Cl^-	4.0	1.9 ± 0.9	4.3	2.2 ± 0.9	–	–		
Gly-Ch^+	5.3	7.8 ± 2.2	5.6	8.8 ± 1.4	–	–		
Ch^+-Cl^-	4.4	3.4 ± 1.2	4.7	3.8 ± 0.9	–	–		
Ch^+-Ch^+	6.3	3.9 ± 1.6	6.4	4.0 ± 1.3	–	–		
Cl^--Cl^-	7.5	9.1 ± 2.2	7.7	11.0 ± 1.8	–	–		
AcPh-Ch^+	5.5	3.7 ± 1.4	6.4	4.9 ± 1.2	–	–		
AcPh-Cl^-	5.1	2.4 ± 1.2	6.2	4.2 ± 1.2	–	–		
AcPh-Gly	5.5	7.6 ± 2.1	6.1	9.4 ± 1.2	5.4	14.0 ± 2.0	6.2	13.7 ± 2.4
AcPh-AcPh	5.0	0.2 ± 0.4	4.0	0.04 ± 0.2	5.7	1.2 ± 0.9	4.0	0.07 ± 0.4

The H-bond network was calculated from MD simulations and showed a very similar picture for the pure DES and the 0.2 mmol g^{-1} solution with AcPh (Table 3). The most noticeable difference with the addition of acetophenone was a slight decrease in the number of H-bond between Gly molecules

confirming the preferential interaction of AcPh with Gly. Moreover, the number of Gly-AcPh H-bonds in the DES (0.27 ± 0.09) is found to be much lower than that in pure Gly (0.82 ± 0.14) confirming that in the DES Gly-Ch^+ interactions are preferred over those between Gly and the solute.

Table 3: Average number of H-bonds per acceptor molecule for the pure DES, and a 0.2 mmol g^{-1} solution of acetophenone in DES at 300 K obtained from MD simulations

		Average H-bond number	
Donor	Acceptor	pure DES	0.2 mmol g^{-1} AcPh
Ch^+	Cl^-	0.54 ± 0.02	0.54 ± 0.02
Ch^+	Gly (O)	0.10 ± 0.02	0.10 ± 0.01
Ch^+	AcPh	-	0.03 ± 0.03
Gly	Cl^-	1.89 ± 0.04	1.90 ± 0.05
Gly (HO)	Gly (O)	0.66 ± 0.02	0.65 ± 0.02
Gly (HO)	Ch^+	0.06 ± 0.10	0.05 ± 0.10
Gly	AcPh	-	0.27 ± 0.09

The self-diffusion coefficients of the different components of the DES were calculated from MD with and without AcPh. Both systems show similar results (Table 4), corroborating the idea that the structure of the DES is not perturbed by the presence of AcPh. The highest difference was calculated for Ch^+ which showed a higher diffusion coefficient in the AcPh solution.

Table 4: Diffusion coefficient for a solution of acetophenone in the DES at 300 K obtained from MD simulations. Experimental values for pure DES measured at 298.15 K from D'Agostino et al.[16]

Molecule	Diffusion coefficient $\times 10^{-12}$ m^2 s^{-1}		
	pure DES	0.2 mmol g^{-1} AcPh	expt[16]
Ch^+	3.3 ± 0.2	3.7 ± 0.1	3.8
Cl^-	5.7 ± 0.1	5.6 ± 0.2	
Gly	5.6 ± 0.1	5.8 ± 0.2	5.2
Acetophenone	-	5.6 ± 0.8	

From these results it became clear that there were no special intermolecular interactions in these solutions that might be "activating" the acetophenone substrate during the Grignard reactions. Acetophenone has limited solubility in the ChCl:Gly DES, and there are no distinctly different interactions of glycerol and choline with acetophenone in the DES, compared to those in pure glycerol. Yet, glycerol alone was not an effective solvent for organomagnesium or organolithium additions to

ketones in synthetic experiments.[10] The fact that the Grignard or alkyl-lithium reagents were always added as solutions in an organic solvent, typically an ether, with rapid stirring therefore suggested another route to reaction specificity might be in play. In water, molecules with limited solubility are normally preferentially concentrated at the air- or oil-water interface, to minimize disruption of the water hydrogen bonding network. Therefore, in a H-bonded DES, similar segregation of the sparingly soluble acetophenone to the DES interface would both cause it to be more available for rapid and complete reaction with the Grignard reagent and explain the need for rapid stirring to increase the interfacial area for reaction.

Interfacial Measurements

To test the surface activity hypothesis for acetophenone, surface tension measurements were made of AcPh/DES and AcPh/glycerol solutions (Figure 4). The addition of acetophenone substantially reduced the surface tension at the ChCl:Gly-air interface to 52.4 ± 0.5 mN m^{-1}, compared to the pure DES surface tension of 66.9 ± 0.2 mN m^{-1}. The interfacial tension continued decreasing with concentration until *ca.* 2 wt.% acetophenone, indicating saturation of the surface activity occurring at around 0.2 mmol g^{-1}, corresponding with the limiting solubility measured by NMR above.

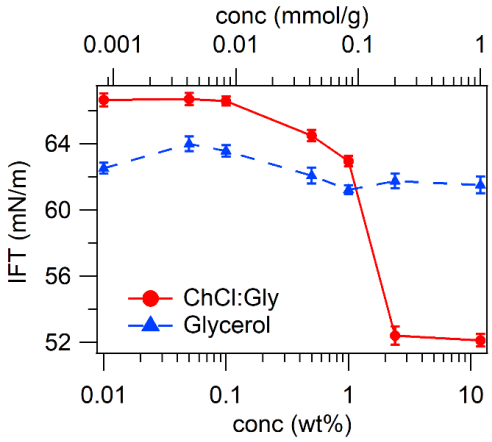

Figure 4: Interfacial tension measured using the drop-shape-analysis method with varying acetophenone concentration in the solvent at the air/ChCl:Gly interface (red) and air/glycerol interface (blue). The data reported is the average value of the measurements with the standard error. The lines are drawn as guide to the eye.

Subsequent MD simulations similarly showed a decrease in surface tension, from 65.0 ± 2.4 mN m^{-1} to 60.3 ± 0.7 mN m^{-1} in the case of the 0.2 mmol g^{-1} solution, with clearly visible accumulation of AcPh at the interface. Conversely, experimental measurements of interfacial tension for acetophenone in pure glycerol (Figure 4) showed little meaningful change (63.2 ± 0.2 mN m^{-1} in pure glycerol and 61.5 ± 0.5

mN m^{-1} for concentrations as high as 1 mmol g^{-1}) indicating no accumulation of acetophenone at the glycerol/air interface.

The interfacial accumulation of acetophenone in ChCl:Gly was therefore studied in more detail using neutron reflectometry. A solid-liquid flow cell containing silicon blocks coated with octadecyltrichlorosilane (OTS) was used to mimic the DES/organic interface more closely than the air-DES interface. Pure DES and a solution of AcPh in the DES were flowed through the system and the interfacial structure was measured. The interface was modelled as a layered structure on the silicon oxide capped silicon substrate, comprising an OTS layer solvated by the DES for the pure DES case and an OTS and AcPh layer solvated by the DES for the solution of DES with AcPh. Details of the neutron reflectivity measurements and modelling are given in Supplementary Information (Section S3). The measured reflectivity profiles and fits of the ChCl:Gly/OTS interface with and without added acetophenone, along with the SLD profile of the fitted interfacial layered structure for the various layers, are shown in Figure 5. The best fit value for the parameters describing the model and their Bayesian posteriors are given in Supplementary Information Figure S9 and Table S5.

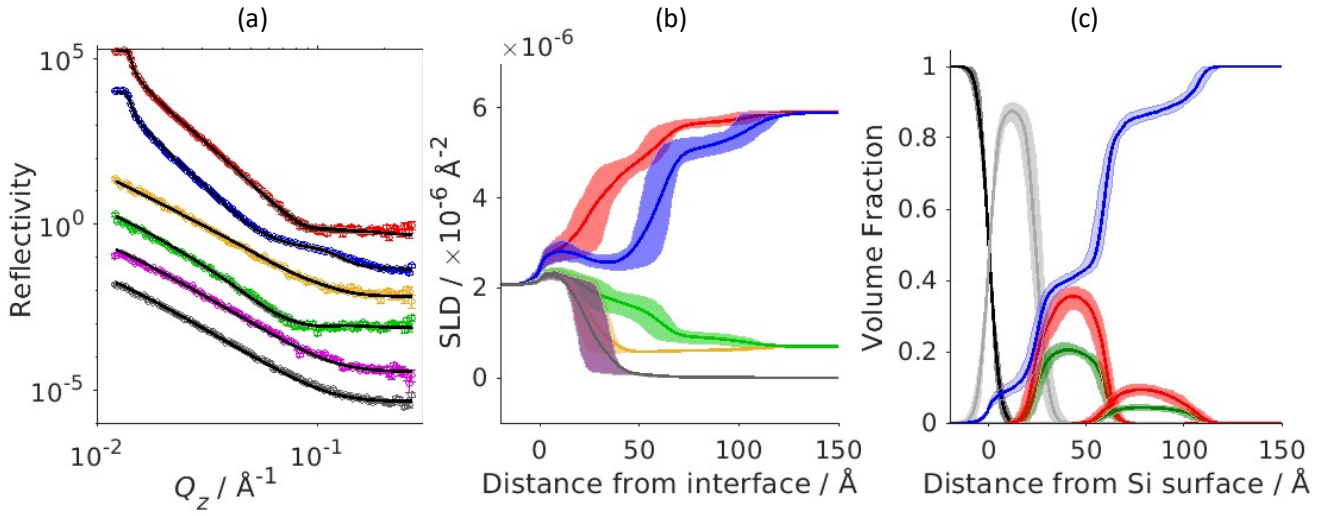

Figure 5: Neutron reflectivity measurements and fits for ChCl:Gly/OTS interface without and with added acetophenone. (a): Reflectivity curves and fitted reflectivity profiles, with the 65% confidence interval, from OTS/air (gray and magenta), OTS/d-DES (red) and OTS/h-DES (yellow), OTS/d-DES+h-AcPh (blue) and OTS/h-DES+d-AcPh (green) interface. (b): The corresponding SLD profiles with a shaded region showing the 65% confidence interval on the fit parameters. (c): The volume fraction distribution of all the components across the interface: silicon (black), silicon oxide (grey), OTS (green), acetophenone (red) and the DES (blue). The shaded region represents the 65% confidence interval on the parameters.

The neutron reflectivity measurements show (see also Supplementary Information Figure S8 and S10) that in the absence of any acetophenone in the DES, the interface comprises a first "dense" OTS layer of thickness 32 Å with an OTS volume fraction Φ_{OTS} = 0.2 and DES volume fraction Φ_{DES} = 0.8, and a second rather "disperse" layer of 41 Å with Φ_{OTS} = 0.05 and Φ_{DES} = 0.95, beyond which pure bulk DES is observed. This second layer of OTS could be silane clusters formed in solution that have deposited onto the silicon block along with the self-assembled monolayer, which if very dilute could also manifest as a second layer. Acetophenone penetrates the first "dense" OTS layer. For the mixtures, the near-surface layer comprises Φ_{OTS} = 0.2, Φ_{AcPh} = 0.4 and Φ_{DES} = 0.4, while the second "disperse" layer now comprises Φ_{OTS} = 0.05, Φ_{AcPh} = 0.1 and Φ_{DES} = 0.85. These experiments provide further evidence that acetophenone forms a surface excess Γ, where the solute is in excess at the interface relative to the bulk. These studies help to explain the observations from the synthetic chemistry, i.e. the need for stirring, and the requirement to use the DES rather than pure glycerol. Our experimental evidence shows that acetophenone segregates to the interface due to its amphiphilicity and partial insolubility in the DES, which provides a framework for understanding the high reactivity and selectivity observed in reactions using these systems.

Finally, a mixed DES/organic system was simulated with classical MD (Figure 6). THF was selected as the organic phase and in addition to the DES/THF mixture, AcPh was added at two concentrations: 0.2 mmol/g and 1.0 mmol/g (see the Methods section for a more exhaustive description). The interfacial region was selected according to the area where the THF density went from 90% to 10% of its bulk value. This corresponds to two zones: one that is located approximately at the central area of the box, and a second that encompasses the extremities. Due to the annealing procedure and the different composition of the three simulated systems the absolute position of the interface was found to be slightly different in each simulation.

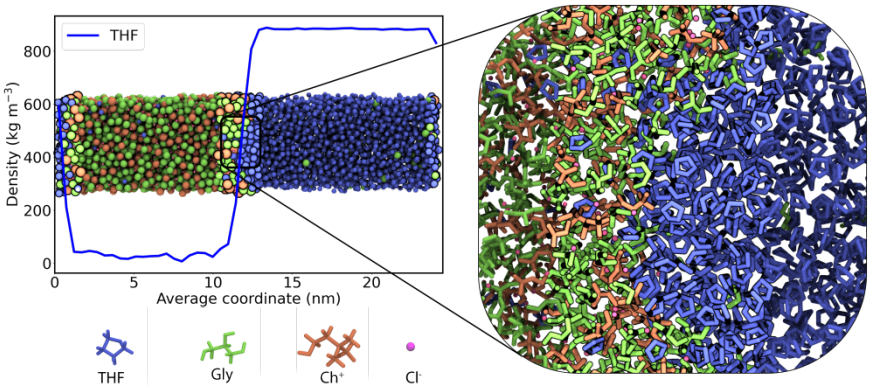

Figure 6: The mixed DES/THF model. Molecules are represented as beads located at their centre of mass. The highlighted regions correspond to the interface at the beginning of production runs, displayed in detail in the inset.

During production simulations, AcPh was not homogeneously distributed in the DES, whereas in THF the density profile was seen to be more regular. Noticeably, for both concentrations of AcPh, progressing along the simulation, an increasing number of acetophenone molecules became localized in the THF region, as shown by the average number of molecules obtained from the integrated density profiles. Another indication that the AcPh were migrating to the THF phase was seen when calculating RDFs between the centres of mass of AcPh and THF at different simulation times (Supporting Information Figure S11). Integration of the RDFs until the first minimum over the initial 50ns interval returned a coordination number of ~10 THF molecules to AcPh for both concentrations. In the last interval, after 450-500ns, that number increased to ~12 molecules. It was also observed that the shape of the functions remained unaltered, whereas only their values increased at later stages in the simulations, meaning that the increase is not caused by a change in the interactions between the two molecules but, by the fact that on average more AcPh is found in bulk THF.

Quantitative analysis of the free energy of the transfer of AcPh from the DES to the organic phase was conducted employing umbrella sampling (US) simulations (see the Methods section for full details), transferring AcPh from the bulk DES to the bulk THF phase. In the bulk DES, the calculated free energy profile was irregular. This is likely due to the highly structured nature of the DES, and its high viscosity which translates to much slower relaxation times. Approaching the interfacial region, the free energy decreased, and as soon as AcPh moved into THF it reached its minimum value. Overall, US showed a preference of AcPh for the organic phase of approximately 7.5 kJ/mol (see Supporting Information Figure S12). No relevant local minimum was found in the interface region, hinting at the fact that the composition of the interface is not so relevant to steer the partitioning of AcPh between the two phases.

The last system that was investigated was a DES/THF interface where both AcPh and the Grignard reagent *i*PrMgCl at a concentration of 0.2 mmol/g are initially located in DES and THF, respectively. AcPh was seen to move towards the organic phase from the bulk DES (Figure 7a) and the trajectories showed a clear accumulation of the organometallic species close to the interfacial regions already after the first 50 ns, and an increased presence at later stages (Figure 7b).

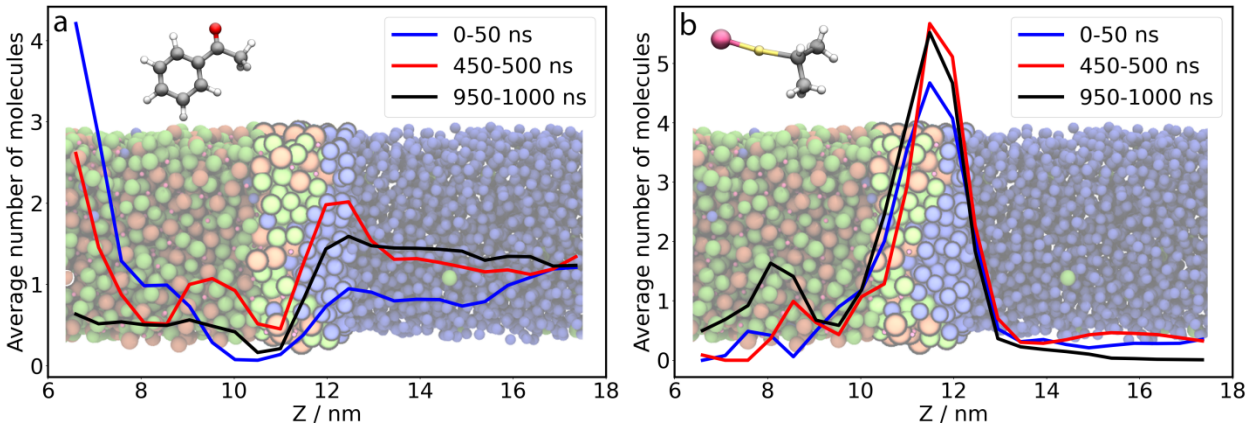

Figure 7: Average number of AcPh (a) and iPrMgCl (b) molecules along the Z coordinate in the mixed DES/THF system at different simulation times.

All simulated systems containing AcPh and DES, demonstrated a similar pattern of intermolecular interactions between between AcPh and the DES components. Two main classes of interactions were observed (Figure 8): the formation of a hydrogen bond between AcPh and Gly and a π-cation interaction between the aromatic rings of AcPh and the positively charged ammonium region of Ch^+. The latter, which is well described,[17, 18] has been seen previously for aromatic solutes in DES containing choline cations.[19] It is analogous to the π-cation interactions found in biological systems[20, 21] such as in transmembrane proteins where aromatic residues are located often at the interface where they can effectively interact with the positively charged heads of membrane phospholipids.[22-25] These Ch^+-AcPh interactions can explain the decrease in surface tension in the DES where the presence of AcPh molecules shield the surface from the less favorable interactions with air or THF.

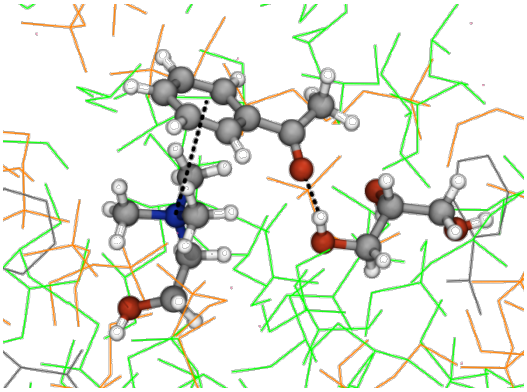

Figure 8: Non-covalent interactions between AcPh, Gly and Ch^+ at DES interface, identified during MD. H-bonding with Gly and π-cation interactions with Ch^+ are evidenced by dotted lines. Surrounding DES is represented in lines, with colour code: Ch+: orange; Gly: green; AcPh: grey.

Discussion

The potential improvements DES can offer for organometallic chemistry[26] prompted us to seek a clearer understanding of the structural details of these solvents and their solutions of organic substrates and organometallic reagents. Our simulations and new experimental data match previous reports on the pure DES structure,[13] within uncertainties. The measured and computed RDFs further confirm that the structure of ChCl:Gly (1:2) is largely driven by the network of H-bonds between glycerol molecules with choline, which contributes to the highly organized structure of the DES. Chloride is accommodated within this network, and both Ch^+ and Cl^- interact with glycerol separately as there was no evidence of strong choline OH group correlations with glycerol OH.[13]

NMR measurements showed that AcPh has relatively low solubility in the DES (see Supporting Information) and the addition of AcPh to the DES did not affect the structural features of the solvent, as confirmed by unaltered experimental and simulated RDFs. The strongest associations are seen between AcPh and Gly followed by Ch^+ and Cl^-. Previous synthetic work had hypothesized that a direct interaction between AcPh and Ch^+ could "activate" the AcPh for reaction.[9, 10] However, there does not appear to be any specific interaction between AcPh and Ch^+ apparent in the experimental scattering results that could result in such activation. Our MD results show further nuance: in the presence of Ch^+ the network of H-bonds that stabilise AcPh in pure Gly is disrupted in favour of choline-glycerol interactions. This makes the DES a poorer solvent for AcPh, despite the formation of Ch^+-AcPh π-cation adducts. We did not observe significant reduction in the surface tension for AcPh in pure Gly, suggesting that the change in H-bonding properties for AcPh displayed in the DES have a major contribution to surface accumulation. Noticeably, when AcPh approaches the interface, stabilization of the otherwise exposed electrostatic

charge of choline through π-cation interactions, as observed in our simulations, would lower the chemical potential of the surfacing choline, thus contributing to the decrease of the surface tension, as measured in the experiment data.

Probing AcPh in more 'realistic' biphasic DES/organic mixtures with neutron reflectivity revealed a 1 nm layer of AcPh between the DES and the solid (OTS-coated) phase, confirming the tendency of this aromatic ketone to prefer low polarity environments. Evolution of the density profiles (Figure 7) and RDFs (Figure 8) in MD simulations for the mixed DES/THF system also showed partitioning of AcPh towards the organic phase. The free energy of the preference of AcPh for the organic phase was calculated with umbrella sampling and clearly showed a stabilization of AcPh by approximately 7 kJ/mol when going from the DES to THF. Lastly, the addition of an organometallic reagent (^{i}PrMgCl) to the THF phase caused no changes in the behaviour of AcPh. Interestingly, also ^{i}PrMgCl showed a non-uniform distribution in the DES/THF mixture with an even more clear accumulation than AcPh at the interface, probably due to the favourable interaction that can be created between the highly polarized Mg-Cl bond and the ionic pair Ch^{+}-Cl^{-}.

Thus, from this evidence we suggest that the reaction of ketones in deep eutectic solvents with organometallic reagents is an interfacial reaction, with specificity resulting from orientation of the ketone and the organometallic species at the interface. This also explains the increased rate of the reaction, due to the localization of higher concentrations of the reactive species at the interface, precisely where they will easily encounter each other. It also explains why the organometallic reagent does not react immediately with the DES components, as they are at a lower concentration at the interface than the substrate. We note that interfacial activity has also been seen in our recent experimental work on similar systems, for other ketones in DES[27] and also for phenyl lithium reagents in DES-organic solvent mixtures in flow,[28] in addition to the acetophenone solutions and ^{i}PrMgCl reagent studied in greater detail here.

Conclusions

Using DES as the solvent for the substrate in polar organometallic reactions offers drastic improvements in yields and selectivity. In this work we have analysed the structure of a DES composed of a 1:2 molar ratio of choline chloride and glycerol in presence of an aromatic ketone, acetophenone, as a typical substrate for an organolithium or organomagnesium reaction. Wide angle neutron scattering, NMR, tensiometry and neutron reflectivity paired with classical all-atom molecular dynamics simulations allowed the thorough investigation of the DES in the presence and absence of AcPh, and the behaviour of the latter in the DES and in a mixed DES/organic phase. Structural characterization of the

DES shows a clear network of H-bond interactions between choline and glycerol in which chloride anions are accommodated. However, surprisingly the solubility of acetophenone in the DES is limited and no substantial structural changes between solvent component interactions were observed in solutions containing the ketone.

Instead, both experiments and calculations agree that there is a tendency for acetophenone to accumulate at the DES/air interface. In the presence of an organic phase in mixed DES/organic systems, neutron reflectivity showed that a layer of acetophenone forms between the DES and an organosilane-coated solid phase while MD simulations revealed the tendency of acetophenone to move towards the organic phase in a DES/THF system. Finally, preliminary calculations on a mixed DES/THF system containing ^{i}PrMgCl showed that the latter is unevenly distributed in this mixed system and also tends to accumulate at the interface.

All the evidence stemming from experiment and calculations points to the role of the DES being to organise the acetophenone substrate at the surface of this solvent, where it is primed to react with the organometallic species. There are no strong specific chemical interactions between any component of the DES with the substrate which could enhance the reactivity of specific bonds in this species, compared to any others in the solution. Instead, the presence of polar choline chloride in glycerol makes this mixture a less favourable environment for solubilization of the less polar acetophenone, than in pure glycerol. In the DES, acetophenone accumulates at the interface, giving a surface excess of the substrate. When an apolar solvent is added, acetophenone can rapidly move into the organic phase without the need to diffuse through the highly viscous DES, facilitating faster reactions and also protecting sensitive reagents from protic solvent components which will be relatively depleted at the same interface. A similar behaviour was also seen for ^{i}PrMgCl, a model organometallic reagent, for which accumulation at the interface was revealed. In conclusion, acetophenone is interfacially active in the investigated DES which, when combined with an organic phase, could have a synergistic effect on the substrate and reagent both toward the activation of organometallic reactions.

This conclusion means that such selectivity and improved yields need not be restricted to DES-based reaction systems but could also be used to engineer reaction systems using other solvent pairs by adjusting the relative solubility of the substrate to favour interfacial accumulation. We note that other work has demonstrated the use of aqueous solutions for an "on-water" based reaction system.[5] Also, while neat glycerol can be a suitable solvent for certain substrates in organolithium chemistry,[29] it does not promote selectivity for the ketone studied here. We predict that, in cases where the substrate is largely insoluble, studies of the air-solvent surface tension, in the presence of the required substrate, could

provide a quick and simple method to screen water, DES or other solvents for their ability to promote similar interfacial reactions for those particular substrates.

Experimental

Materials

Choline chloride ($(CH_3)_3N(CH_2)_2OHCl$; ChCl; ≥99% chemical purity), glycerol ($HOCH_2CH(OH)CH_2OH$; Gly; ≥99% chemical purity), acetophenone ($CH_3COC_6H_5$; AcPh; 99% chemical purity) and octadecyltrichlorosilane ($CH_3(CH_2)_{17}SiCl_3$; OTS; ≥90% purity) were obtained from Sigma-Aldrich. d_9-choline chloride ($(CD_3)_3N(CH_2)_2OHCl$; d-ChCl; 98 atom-% D), d_8-glycerol ($DOCD_2CD(OD)CD_2OD$; d-Gly; 99 atom-% D) and d_5-acetophenone ($CH_3COC_6D_5$; d-AcPh; 98 atom-% D) were purchased from Cambridge Isotope Laboratories. All chemicals were used as provided. The silicon blocks used for neutron reflectivity were sourced from Crystran Limited.

Sample Preparation

The choline chloride:glycerol (ChCl:Gly) DES was prepared by combining the components in molar ratios of 1:2. The mixtures were stirred at 60 °C until a clear, homogeneous liquid was obtained, which was subsequently sealed and equilibrated overnight. Acetophenone was dissolved in the DES by vigorous magnetic stirring at room temperature at different concentrations (0.0008 – 1 mmol g^{-1}) for tensiometry experiments or different isotopically labelled contrasts in saturated solutions for liquid neutron diffraction and reflectometry measurements.

Experimental measurements

To quantify the solubility of acetophenone in ChCl:Gly DES and in glycerol, ^{1}H NMR spectra were acquired at 298 K on a Bruker Neo500 spectrometer operating at 500.13 MHz, using 4 scans, 30-degree pulses, and a 60 second delay between pulses to help ensure accurate quantitation.

Liquid neutron diffraction experiments were performed using the NIMROD diffractometer[30] at ISIS Pulsed Neutron and Muon Source, UK (RB1820315[31]). Using time-of-flight (TOF) neutrons with wavelength $0.05 \leq \lambda \leq 11$ Å and detectors spanning the angular range 0.5 – 40°, a Q-range of $0.01 \leq Q \leq 50$ Å^{-1} was obtained. Pure DES samples were prepared and measured at 6 different isotopically labelled contrasts for liquid neutron diffraction experiments (see Supplementary information section S2 for details). Acetophenone in DES mixtures were prepared at 1 mmol g^{-1} and measured at the saturated

concentration at 8 isotopically labelled contrasts. In case of acetophenone in glycerol 1 mmol g^{-1} mixtures were prepared and measured at the saturated concentration at 4 isotopically labelled contrasts.

Null-scattering, vacuum-sealed $Ti_{0.68}Zr_{0.32}$ sample cells with a path-length of 1 mm were filled with ~1.5 g of each sample and placed in a sample changer at 298 ± 0.1 K. Measurements were performed using a collimated neutron beam of 30 mm square, with a counting time of 2 – 3 hours. Empty sample cells, the empty instrument, and a 3 mm thick null coherent scattering vanadium niobium standard were measured for data normalisation and instrument calibration. Data were corrected and normalised using GudrunN software.[32]

After correction for hydrogen inelasticity,[33] the reduced data were analysed using Empirical Potential Structure Refinement (EPSR) modelling,[34-36] a Monte Carlo-derived method, that uses the experimental diffraction data to constrain a molecular model. For the choline chloride:glycerol DES, 200 choline, 200 chloride and 400 glycerol molecules were added to a simulation box of 45 $Å^3$ with an atomic density of 0.11 atom $Å^{-3}$. In case of ChCl:Gly DES with acetophenone, 200 choline, 200 chloride, 400 glycerol and 14 acetophenone molecules in a box of 45.3 $Å^3$ with the same atomic density were used, and in the case of glycerol with acetophenone, 400 glycerol and 37 acetophenone molecules were taken in a box of 45.3 $Å^3$ with an atomic density of 0.112 atom $Å^{-3}$. The required number of acetophenone molecules was calculated from the concentration in each system, as determined by NMR.

Surface tension measurements were made at room temperature (21 °C) using the drop-shape-analysis method[37] with a FTA1000 Drop Shape Analyser. Concentration series of the acetophenone in DES and acetophenone in glycerol ranging from 0.0008 – 1 mmol g^{-1} (0.01 – 12 wt %) were prepared and measured at room temperature. The surface tension at each concentration was measured 3 – 4 times using a fresh drop, with each measurement comprising 100 data points taken within 1 min. The data reported is the average value of the measurements with the standard error.

Neutron reflectivity, on a model system consisting of a hydrophobic OTS layer supported on silicon blocks, exposed to the solutions of ChCl:gly, was measured on the OFFSPEC reflectometer[38] at ISIS Pulsed Neutron and Muon Source, UK (experiment number RB2010710[39]). Using time-of-flight (TOF) neutrons with wavelengths $1.0 \leq \lambda \leq 14$ Å and incidence angles of 0.7° and 2.0°, a Q-range of $0.012 \leq Q \leq 0.27$ $Å^{-1}$ was obtained.

Silicon blocks for reflectivity were coated with an OTS layer, which mimics the hydrophobic interface that is present in the reaction more closely than air, using the procedure described by Brzoska et al[40] (see Supplementary information section S3 for details). The OTS coated silicon blocks were sealed into a solid-liquid reflectivity flow cells through which the ChCl:Gly DES was flowed, without and with the

acetophenone. Measurements were done at three contrasts of ChCl:Gly DES and AcPh: d-AcPh in h-ChCl:h-Gly (h-DES), h-AcPh in d-ChCl:d-Gly (d-DES) and d-AcPh in d-ChCl:d-Gly (d-DES). The layered structure and SLD were used to co-refine the multiple neutron reflectivity contrasts using the RasCAL fitting routine,[41] allowing for determination of the presence and penetration of acetophenone at the solvent/OTS boundary and giving molecular details of the interfacial layer. Confidence bands on the fit parameters and the structure were determined using RasCAL's inbuilt Bayesian analysis function.

Molecular Dynamics

The modelling study was conducted employing classical all-atom molecular dynamics (MD) in GROMACS 2023-dev.[42] Atomic charges and force field parameters for Gly and ChCl were taken from the literature,[43] whereas for THF a RESP fit of HF/6-31G* electrostatic potential provided the atomic charges and the standard GAFF[44] parameters were used for bonded interactions. The DES systems were modelled as a 1:2 ChCl:Gly solution in cubic 60 Å boxes, containing 800 Gly and 400 ChCl molecules. The AcPh solution in pure DES at a concentration of 0.2 mmol g^{-1} was obtained adding 26 AcPh molecules to the above-mentioned system. The interface system was modelled as a rectangular box of 60 × 60 × 250 Å in which the DES components (1668 Gly molecules and 834 ChCl molecules) were placed in the first half of the box along the Z axis and the rest was completed by 3337 THF molecules. Two solutions of AcPh in the DES/THF systems were modelled: one at a concentration of 0.2 mmol g^{-1} (adding 102 molecules of AcPh randomly distributed between the two phases) and a second at 1.0 mmol g^{-1} (adding 511 molecules of AcPh randomly distributed between the two phases). Finally, a system containing 54 molecules of AcPh and 54 molecules of *i*PrMgCl distributed in the DES and THF phases respectively was created to mimic a complete organometallic reaction environment. After steepest-descent energy minimization with a maximum force tolerance threshold of 200 kJ mol^{-1} nm^{-1}, molecular dynamics simulations were conducted in the NPT ensemble at 300 K using a stochastic velocity and box rescaling algorithm.[45] Bonds involving H atoms were constrained using the LINCS algorithm[46] and the selected timestep was 2 fs. For the mixed DES/THF systems, an initial 1 ns equilibration in which a semi-isotropic barostat was employed, accounted for the relaxation of the surface tension between the two immiscible phases. Due to the high viscosity of the DES a 10 ns annealing procedure was carried out, going from 300 to 500 K in 1 ns cycles, followed by 500 ns of production simulations for the pure Gly, pure DES and AcPh solutions in DES. In case of the mixed DES/THF systems where both AcPh and iPrMgCl are present, production runs were extended to 1000 ns. Diffusion coefficients were calculated starting from mean squared displacements from 10 to 100 ns after checking that the system reached the diffusive regime in that window.[47] The systems containing only DES and DES plus AcPh were simulated

for additional 50 ns at constant volume, after increasing the simulation box in the Z direction by a factor of 6, to simulate the DES/air interface. To ensure the equilibration of these systems, for the first 25 ns of the NVT simulation an annealing procedure was used taking the temperature from 300 K to 500 K and back in 5 ns cycles.

Umbrella sampling simulations

Umbrella sampling (US)[48] was used to study the transfer of AcPh from the DES to the organic phase. The windows for US were prepared by extracting 21 snapshots from a short simulation in which a harmonic potential of 2000 kJ mol^{-1} nm^{-1} was applied between the centre of mass of a specific AcPh molecule and that of the choline residues. The extracted snapshots were selected to span a range of positions that went from DES bulk to THF bulk. The applied force constant in each of the windows was 200 kJ mol^{-1} nm^{-1} and a simulation time of 30 ns in the NPT ensemble at 300 K and 1 atm with was chosen to allow an exhaustive sampling of the bulk DES windows. Free energy profiles were obtained through the Weighted Histogram Analysis Method (WHAM) as implemented in the GROMACS package, discarding the first 6 ps of each window.

ASSOCIATED CONTENT

Supplementary Information Available: NMR measurements on acetophenone solubility in different solvents, experimental details for neutron diffraction and neutron reflectivity measurements, detailed analysis of neutron diffraction and neutron reflectivity data, THF-AcPh centre of mass radial distribution functions, free energy profile for the transfer of an AcPh molecule from DES to THF.

AUTHOR INFORMATION

Corresponding Authors: Karen J Edler karen.edler@chem.lu.se, Michele Cascella michele.cascella@kjemi.uio.no

Funding Sources

I.M and K.J.E received funding from the EPSRC (Grant Number EP/S020772/1). M.B., M.C., O.E. acknowledge the support of the Research Council of Norway through the Centre of Excellence Hylleraas Centre for Quantum Molecular Sciences (Grant Number 262695) and the Pioneer Research Grant MetalSynergy (Grant Number 314009), and of the Norwegian Supercomputing Program (NOTUR) for computing hours and storage facilities (Grant Numbers NN4654K, NS4654K). M.B. also acknowledges

the support of the European Commission through the MSCA-IF RATIO (Grant Number 101059679) and the EURO-HPC JU (Grant Number EHPC-REG-2023R02-064).

ACKNOWLEDGEMENTS

We thank the ISIS Neutron and Muon Source for the award of neutron beamtime (experiments RB1820315 and RB2010710). We thank Dr Luke Clifton (ISIS Neutron & Muon Source) for his help with creating the appropriate graphs from the neutron data analysis.

References

1. Abranches, D. O.; Coutinho, J. A. P., Everything You Wanted to Know about Deep Eutectic Solvents but Were Afraid to Be Told. *Ann Rev Chem Biomol Eng* **2023,** *14* (1), 141-163.

2. Zhang, Q.; De Oliveira Vigier, K.; Royer, S.; Jerome, F., Deep eutectic solvents: syntheses, properties and applications. *Chem Soc Rev* **2012,** *41* (21), 7108-7146.

3. Kollau, L. J. B. M.; Vis, M.; van den Bruinhorst, A.; Esteves, A. C. C.; Tuinier, R., Quantification of the liquid window of deep eutectic solvents. *Chemical Communications* **2018,** *54* (95), 13351-13354.

4. Hammond, O. S.; Mudring, A.-V., Ionic liquids and deep eutectics as a transformative platform for the synthesis of nanomaterials. *Chemical Communications* **2022,** *58* (24), 3865-3892.

5. García-Álvarez, J.; Hevia, E.; Capriati, V., The Future of Polar Organometallic Chemistry Written in Bio-Based Solvents and Water. *Chemistry – A European Journal* **2018,** *24* (56), 14854-14863.

6. Domingues, L.; Duarte, A. R. C.; Jesus, A. R., How Can Deep Eutectic Systems Promote Greener Processes in Medicinal Chemistry and Drug Discovery? *Pharmaceuticals* **2024,** *17* (2).

7. Celina, G.; Victor, S. M., Asymmetric Addition to Ketones: Enantioselective Formation of Tertiary Alcohols. *Curr. Org. Chem.* **2006,** *10* (14), 1849-1889.

8. Denmark, S. E.; Fu, J., Catalytic Enantioselective Addition of Allylic Organometallic Reagents to Aldehydes and Ketones. *Chem. Rev.* **2003,** *103* (8), 2763-2794.

9. Vidal, C.; García-Álvarez, J.; Hernán-Gómez, A.; Kennedy, A. R.; Hevia, E., Introducing Deep Eutectic Solvents to Polar Organometallic Chemistry: Chemoselective Addition of Organolithium and Grignard Reagents to Ketones in Air. *Angew. Chem. Intl. Ed.* **2014,** *53* (23), 5969-5973.

10. Vidal, C.; García-Álvarez, J.; Hernán-Gómez, A.; Kennedy, A. R.; Hevia, E., Exploiting Deep Eutectic Solvents and Organolithium Reagent Partnerships: Chemoselective Ultrafast Addition to

Imines and Quinolines Under Aerobic Ambient Temperature Conditions. *Angew. Chem. Intl. Ed.* **2016,** *55* (52), 16145-16148.

11. Sánchez-Condado, A.; Carriedo, G. A.; Presa Soto, A.; Rodríguez-Álvarez, M. J.; García-Álvarez, J.; Hevia, E., Organolithium-Initiated Polymerization of Olefins in Deep Eutectic Solvents under Aerobic Conditions. *ChemSusChem* **2019,** *12* (13), 3134-3143.

12. García-Garrido, S. E.; Presa Soto, A.; Hevia, E.; García-Álvarez, J., Advancing Air- and Moisture-Compatible s-Block Organometallic Chemistry Using Sustainable Solvents. *European Journal of Inorganic Chemistry* **2021,** *2021* (31), 3116-3130.

13. Turner, A. H.; Holbrey, J. D., Investigation of glycerol hydrogen-bonding networks in choline chloride/glycerol eutectic-forming liquids using neutron diffraction. *Phys. Chem. Chem. Phys.* **2019,** *21* (39), 21782-21789.

14. Faraone, A.; Wagle, D. V.; Baker, G. A.; Novak, E. C.; Ohl, M.; Reuter, D.; Lunkenheimer, P.; Loidl, A.; Mamontov, E., Glycerol Hydrogen-Bonding Network Dominates Structure and Collective Dynamics in a Deep Eutectic Solvent. *J Phys. Chem. B* **2018,** *122* (3), 1261-1267.

15. Towey, J. J.; Soper, A. K.; Dougan, L., The structure of glycerol in the liquid state: a neutron diffraction study. *Phys. Chem. Chem. Phys.* **2011,** *13* (20), 9397-9406.

16. D'Agostino, C.; Harris, R. C.; Abbott, A. P.; Gladden, L. F.; Mantle, M. D., Molecular motion and ion diffusion in choline chloride based deep eutectic solvents studied by 1H pulsed field gradient NMR spectroscopy. *Physical Chemistry Chemical Physics* **2011,** *13* (48), 21383-21391.

17. Meot-Ner, M.; Deakyne, C. A., Unconventional ionic hydrogen bonds. 2. NH+.cntdot..cntdot..cntdot..pi.. Complexes of onium ions with olefins and benzene derivatives. *Journal of the American Chemical Society* **1985,** *107* (2), 474-479.

18. Biedermann, F.; Schneider, H.-J., Experimental Binding Energies in Supramolecular Complexes. *Chemical Reviews* **2016,** *116* (9), 5216-5300.

19. Hammond, O. S.; Atri, R.; Bowron, D. T.; Edler, K. J., Neutron Diffraction Study of Indole Solvation in Deep Eutectic Systems of Choline Chloride, Malic Acid, and Water. *Chemistry – A European Journal* **2022,** *28*, e202200566.

20. Gallivan, J. P.; Dougherty, D. A., Cation-π interactions in structural biology. *Proceedings of the National Academy of Sciences* **1999,** *96* (17), 9459-9464.

21. Hunter, C. A.; Low, C. M. R.; Rotger, C.; Vinter, J. G.; Zonta, C., Substituent effects on cation–π interactions: A quantitative study. *Proceedings of the National Academy of Sciences* **2002,** *99* (8), 4873-4876.

22. Mbaye, M. N.; Hou, Q.; Basu, S.; Teheux, F.; Pucci, F.; Rooman, M., A comprehensive computational study of amino acid interactions in membrane proteins. *Scientific Reports* **2019,** *9* (1), 12043.

23. Petersen, F. N. R.; Jensen, M. Ø.; Nielsen, C. H., Interfacial Tryptophan Residues: A Role for the Cation-π Effect? *Biophysical Journal* **2005,** *89* (6), 3985-3996.

24. Broemstrup, T.; Reuter, N., How does Proteinase 3 interact with lipid bilayers? *Physical Chemistry Chemical Physics* **2010,** *12* (27), 7487-7496.

25. Waheed, Q.; Khan, H. M.; He, T.; Roberts, M.; Gershenson, A.; Reuter, N., Interfacial Aromatics Mediating Cation−π Interactions with Choline-Containing Lipids Can Contribute as Much to Peripheral Protein Affinity for Membranes as Aromatics Inserted below the Phosphates. *The Journal of Physical Chemistry Letters* **2019,** *10* (14), 3972-3977.

26. Rodríguez-Álvarez, M. J.; Ríos-Lombardía, N.; García-Garrido, S. E.; Concellón, C.; del Amo, V.; Capriati, V.; García-Álvarez, J., Recent Advancements in the Utilization of s-Block Organometallic Reagents in Organic Synthesis with Sustainable Solvents. *Molecules* **2024,** *29* (7).

27. Platten, A. W. J.; Manasi, I.; Campana, M.; Edler, K.; Hevia, E., Harnessing Deep Eutectic Solvents for Regioselective Polar Additions to α,βUnsaturated Ketones and Aldehydes. *ChemSusChem* **2024,** *n/a* (n/a), e202402083.

28. Mulks, F. F.; Pinho, B.; Platten, A. W. J.; Andalibi, M. R.; Expósito, A. J.; Edler, K. J.; Hevia, E.; Torrente-Murciano, L., Continuous, stable, and safe organometallic reactions in flow at room temperature assisted by deep eutectic solvents. *Chem* **2022,** *8* (12), 3382-3394.

29. Rodríguez-Álvarez, M. J.; García-Álvarez, J.; Uzelac, M.; Fairley, M.; O'Hara, C. T.; Hevia, E., Introducing Glycerol as a Sustainable Solvent to Organolithium Chemistry: Ultrafast Chemoselective Addition of Aryllithium Reagents to Nitriles under Air and at Ambient Temperature. *Chemistry – A European Journal* **2017,** *24* (7), 1720-1725.

30. Bowron, D. T.; Soper, A. K.; Jones, K.; Ansell, S.; Birch, S.; Norris, J.; Perrott, L.; Riedel, D.; Rhodes, N. J.; Wakefield, S. R.; Botti, A.; Ricci, M.-A.; Grazzi, F.; Zoppi, M. , NIMROD: The Near and InterMediate Range Order Diffractometer of the ISIS second target station. *Rev. Sci. Instru.* **2010,** *81*, 033905.

31. Edler, K. J.; Atri, R.; Holbrey, J. D.; Bowron, D. T.; Hammond, O. S.; Hooton, J.; Hevia, E., Deep Eutectic Solvents in Chemical Synthesis: Probing Solvent-Substrate Interactions, STFC ISIS Neutron and Muon Source, https://doi.org/10.5286/ISIS.E.RB1820315. 2018.

32. Soper, A. K. *GudrunN and GudrunX: Programs for Correcting Raw Neutron and X-Ray Diffraction Data to Differential Scattering Cross Section. RAL-TR-2011-013*; 2011.

33. Soper, A. K., Inelasticity corrections for time-of-flight and fixed wavelength neutron diffraction experiments. *Molecular Physics* **2009,** *107* (16), 1667-1684.

34. Soper, A. K., Empirical potential Monte Carlo simulation of fluid structure. *Chemical Physics* **1996,** *202* (2–3), 295-306.

35. Soper, A. K., Tests of the empirical potential structure refinement method and a new method of application to neutron diffraction data on water. *Molecular Physics* **2001,** *99* (17), 1503-1516.

36. Soper, A. K., Partial structure factors from disordered materials diffraction data: An approach using empirical potential structure refinement. *Phys. Rev. B* **2005,** *72* (10), 104204.

37. Berry, J. D.; Neeson, M. J.; Dagastine, R. R.; Chan, D. Y. C.; Tabor, R. F., Measurement of surface and interfacial tension using pendant drop tensiometry. *J Colloid Interface Sci* **2015,** *454*, 226-237.

38. Dalgliesh, R. M.; Langridge, S.; Plomp, J.; de Haan, V. O.; van Well, A. A., Offspec, the ISIS spin-echo reflectometer. *Physica B: Condensed Matter* **2011,** *406* (12), 2346-2349.

39. Edler, K. J.; Neville, G. M.; Campana, M.; Bathke, E. K.; Manasi, I.; Leaman, N.; Arnold, T.; Hooton, J., Interfacial Chemical Reactions in Deep Eutectic Solvents, STFC ISIS Neutron and Muon Source, https://doi.org/10.5286/ISIS.E.RB2010710-2. 2021.

40. Brzoska, J. B.; Ben Azouz, I.; Rondelez, F., Silanization of solid substrates: A step toward reproducibility. *Langmuir* **1994,** *10* (11), 4367-4373.

41. Hughes, A. RasCAL. https://sourceforge.net/projects/rscl/.

42. Abraham, M. J.; Murtola, T.; Schulz, R.; Páll, S.; Smith, J. C.; Hess, B.; Lindahl, E., GROMACS: High performance molecular simulations through multi-level parallelism from laptops to supercomputers. *SoftwareX* **2015,** *1-2*, 19-25.

43. Perkins, S. L.; Painter, P.; Colina, C. M., Experimental and Computational Studies of Choline Chloride-Based Deep Eutectic Solvents. *Journal of Chemical & Engineering Data* **2014,** *59* (11), 3652-3662.

44. Wang, J.; Wolf, R. M.; Caldwell, J. W.; Kollman, P. A.; Case, D. A., Development and testing of a general amber force field. *Journal of Computational Chemistry* **2004,** *25* (9), 1157-1174.

45. Bussi, G.; Donadio, D.; Parrinello, M., Canonical sampling through velocity rescaling. *The Journal of Chemical Physics* **2007,** *126* (1), 014101.

46. Hess, B.; Bekker, H.; Berendsen, H. J. C.; Fraaije, J. G. E. M., LINCS: A linear constraint solver for molecular simulations. *Journal of Computational Chemistry* **1997,** *18* (12), 1463-1472.

47. Del Pópolo, M. G.; Voth, G. A., On the Structure and Dynamics of Ionic Liquids. *The Journal of Physical Chemistry B* **2004,** *108* (5), 1744-1752.

48. Torrie, G. M.; Valleau, J. P., Nonphysical sampling distributions in Monte Carlo free-energy estimation: Umbrella sampling. *Journal of Computational Physics* **1977,** *23* (2), 187-199.

Table of Contents Figure